JOURNAL OF CATALYSIS 37, 432–448 (1975)

# Experimental Studies of Sintering of Supported Platinum Catalysts

PETER C. FLYNN[1] AND SIEGHARD E. WANKE[2]

*Department of Chemical Engineering, The University of Alberta, Edmonton, Alberta, Canada*

Received August 16, 1974

Changes in the dispersion of supported $Pt/Al_2O_3$ catalysts following reduction and a variety of thermal treatments have been monitored by gas uptake and electron microscopy. Evidence of redispersion was found after sintering of one catalyst in oxygen at 450 to 600°C. Sintering was found to be sensitive to gas atmosphere and metal loading. Addition of a portion of presintered catalyst containing large Pt particles increased the rate of sintering of a catalyst.

From electron micrographs of the same catalyst area before reduction and after reduction and various thermal treatments, it was concluded that Pt agglomeration occurs during all these steps. Some Pt crystallites remain in a fixed location during reduction and thermal treatments.

## INTRODUCTION

Supported metal catalysts show changes in metal surface area during use or treatment at high temperatures. This process is known as sintering, and is of concern industrially because a loss of catalytic activity generally occurs, associated with an increase in the particle size of the metal. A number of patents have been issued for processes designed to redisperse sintered catalysts [see for example, Refs. (*1*,*2*)].

A number of investigators have studied catalyst systems under treatment conditions leading to sintering. In this paper their work is briefly reviewed, and our own experiments are described. From this data the sintering process appears to be extremely complex, and further experiments will be necessary to establish the critical parameters in this process.

[1] Present address: Syncrude Canada Ltd., Edmonton, Alberta, Can.

[2] To whom enquiries concerning this paper should be addressed.

Many authors (*3–10*), in trying to describe the kinetics of sintering, have fitted data to the simple power law equation of the form

$$\frac{ds}{dt} = -Ks^n, \qquad (1)$$

where $s$ is the metal surface, $n$ is generally reported as an integer, and an activation energy is lumped in the constant $K$. Both Herrmann *et al.* (*3*) and Maat and Moscou (*4*) report $n$ values of 2 for $Pt/Al_2O_3$ catalysts in oxidizing environments. The latter authors examined their samples under the electron microscope before and after sintering. Initially the Pt in their catalysts consisted of particles in the 1 nm range. After treatment in air, they reported the presence of 1 to 50 nm particles. Somorjai (*5*) studied supported Pt catalysts sintered in an oxidizing atmosphere by small angle X-ray scattering. Based on data obtained by this technique, he proposed a modified growth law similar to that advanced by Wynblatt and Gjostein (*6*), of the same form as Eq. (1) but with a $K$

value which decreases exponentially with increasing average particle radius $r$, i.e.,

$$K = B \exp(-Ar/RT), \qquad (2)$$

where $A$ and $B$ are constants. Somorjai (*5*) also estimated the activation energy to be 52 kcal for oxidizing atmospheres. However, small angle X-ray diffraction is not equally sensitive to all sizes of Pt particles.

Sintering kinetics change in a reducing environment, in general associated with a higher value of $n$. Somorjai (*5*) found a lower activation energy for an $H_2$ atmosphere, about 20 kcal, but a much lower preexponential factor, and hence a lower overall rate of sintering compared to an oxidizing atmosphere. Gruber (*7*) and Hughes *et al.* (*8*) found $n$ values in the 6 to 8 range for sintering at 500°C in the $H_2$ atmospheres.

Finally, two special studies have been made of $Pt/Al_2O_3$ systems. Wynblatt and Gjostein (*6,9*) used electron microscopy to study Pt particles prepared on specially thin (10 nm) alumina substrates. They found minimal surface migration for a sample where Pt particles were larger than 5 nm, and cite interparticle transport for a mechanism in these and larger Pt particles. High values of $n$ ($>8$) are attributed to facet inhibited growth, i.e., expansion of a Pt particle must await nucleation of a ledge on a smooth face. Experimentally they observed $n$ values from about 3 to 13 for sintering in air. Huang and Li (*10*) studied Ostwald ripening for large ($>100$ nm) Pt particles on $\alpha$-$Al_2O_3$. Their $n$ value of the order of 5 led them to conclude that surface diffusion is the mechanism of the growth process. Gregg and Howlett (*11*) similarly concluded that surface diffusion was the agglomeration process for the sintering of metal spheres observed under the optical microscope. Both Wynblatt and Gjostein (*9*) and Huang and Li (*10*) observed that the sintering rate increased with increases in oxygen concentration in an $O_2/N_2$ mixture.

Two models have been developed to account for particle size changes occurring during sintering. Ruckenstein and Pulvermacher (*12,13*) postulated crystallite migration and collision as a sintering mechanism and developed and solved a model for homogeneous and partially heterogeneous surfaces. This model can account for power law orders of $\geq 2$ ($n = 2$ or 3 for fusion of particles rate controlling, and $n \geq 4$ for diffusion of particles rate controlling). It also predicts that after a certain time a universal dimensionless curve will fit the particle size distribution of a catalyst. Flynn and Wanke (*14,15*) postulated the loss from particles of atomic or molecular metal species, followed by surface diffusion and recapture, as the sintering mechanism. This model can account for power law orders less than zero (i.e., redispersion) up to 13 and higher. The order is found to depend heavily on the nature of the particle size distribution. While under either model the decrease in surface energy provides the driving force for metal agglomeration, the difference between transport as a crystallite or as an atomic species leads to significant differences in predicted growth kinetics. This point is discussed in further detail below in conjunction with some experimental results.

## EXPERIMENTAL METHODS

Four catalysts were used in this work, two commercial catalysts and two prepared in this laboratory. The commercial catalysts were Engelhard 0.3 and 0.5% Pt by weight on alumina pellets. The prepared catalysts were 2.03 and 4.76% Pt by weight on Alon alumina (Cabot Corp.). This substrate is particularly good for electron microscopy specimens since it crushes readily to form thin clumps (*16*). The catalysts were made by adding an appropriate amount of $H_2PtCl_6$ solution to a slurry of Alon and evaporating to dryness (110°C). The specimens were sub-

sequently reduced in flowing hydrogen at 500°C unless the unreduced catalyst was to be examined.

Catalyst samples were characterized by gas uptake measurements and/or electron microscopy. Hydrogen and oxygen uptakes were measured after reduction in flowing hydrogen and outgassing in flowing helium at 500°C for 1 or 2 hr. The conventional flow system used to record uptakes has been previously described (*17*); it also permitted sintering treatments in flowing oxygen or helium. For such cases the time of sintering treatment was measured from the point when the catalyst was placed in the cool furnace, which had a heatup rate of 500°C/hr.

Conventional copper grids covered with a "holey" carbon film were used for specimens not treated after mounting on the grid. Details of grid and specimen preparation and the microscope used are also described in an earlier work (*16*). Micrographs were generally recorded at a magnification of $3.3 \times 10^5$ on the negative; a further magnification of about 3 was realized in printing.

Some micrographs were recorded of catalysts which had been treated on the grid, in order to allow the same specimen area to be examined before and after reduction and thermal treatment. For such cases a tungsten grid was used, to minimize any possible migration of metal from the grid itself. The grid was mounted on a "holey" plastic film prepared in the standard fashion by wetting a thin film of dissolved plastic (*16*). Subsequently, the grid was carbon coated, and the plastic was dissolved away by immersing the grid back into the solvent, leaving only the holey carbon film on the grid. Removal of the plastic layer reduced buckling and movement of the film during heating. The grid was then recoated with carbon, resulting in a thickened holey carbon film with reasonable thermal stability. While such grids could not be treated in oxygen at typical sintering temperatures (500°C), we found that reductions in hydrogen at 300°C never destroyed the film, and sintering treatments in helium at 500 to 600°C did not destroy the film in the region of interest in about 30% of the sintering trials. The unreduced catalyst for these runs, 2.03% Pt on Alon was crushed and suspended in a nondissolving liquid ($CCl_4$) and dropped on the grids. All treatments were carried out in the flow system described above.

## RESULTS

Four series of experiments were conducted to explore the sintering behavior of supported Pt catalysts. In one series catalysts were sintered at varying temperatures for a fixed time period. In a second series, the temperature was fixed and the time of sintering varied. In a third set of runs the sintering behavior of a catalyst batch into which a portion of presintered catalyst containing large Pt particles was mixed was compared to that of an unmixed catalyst. Finally, electron micrographs were recorded of the same catalyst specimen area before and after reduction and sintering in an inert atmosphere.

### *1. Constant Time/Variable Temperature Treatments*

Both commercial catalyst samples (Engelhard 0.5% Pt on $Al_2O_3$) and prepared specimens (4.76% Pt on Alon $Al_2O_3$) were heated 16 hr in oxygen at varying temperatures, and the dispersion or particle size were measured. In the case of the prepared catalyst, small samples ($<0.5$ g) were used, and the progress of sintering was checked by electron micrographs. For the commercial catalyst, batches of sufficient size (8–10 g) were used to allow gas uptakes to be measured after sintering.

Figure 1 shows the size range of particles observed in the micrographs of several specimen areas of the Alon supported catalyst. The lower limit of 1 nm shown in

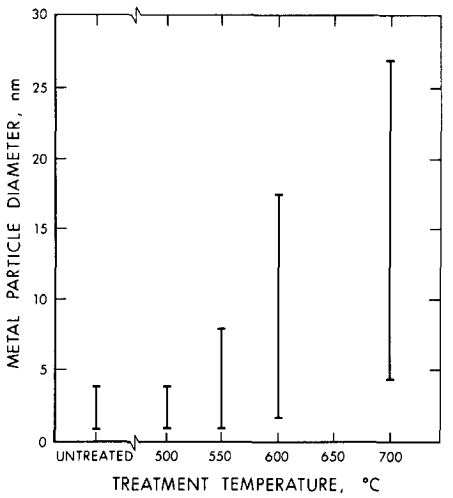


FIG. 1. Effect of treatment temperature on metal particle size range, measured from electron micrographs. Batches of a 4.76% Pt on Alon catalyst were heated 16 hr in flowing oxygen at the indicated temperature.

Fig. 1 is considered the minimum size where metal size contrast can accurately be distinguished from the contrast inherent in the support (*16*). Significant particle growth was observed for 16 hr treatment at 550°C, and for all higher temperatures. For the specimens sintered at 600 and 700°C, particle growth was sufficiently great to significantly lower the number of particles in a given field of view, hence the size ranges for these two cases, based on about five fields of view, must be considered approximate. [Micrographs from this series of experiments have already been published (*14*).] It is clear that the platinum particles grow to the same order of magnitude as the particles in the support (10–30 nm), a point which is discussed further below.

Figure 2 shows the variation of metal dispersion with treatment temperature for the 0.5% Pt commercial catalyst as measured by hydrogen and oxygen uptake at 0°C. The open triangles in Fig. 2 show oxygen uptakes for the same catalyst sample, which was successively sintered overnight in flowing oxygen at 500, 600 and 700°C. The circles in Fig. 2 show oxygen uptakes (open circles) and hydrogen uptakes (solid circles) for separate batches of catalyst sintered at the indicated temperatures. The catalysts were reduced by cooling or heating in flowing hydrogen from the indicated sintering temperature to 500°C; the sole exception was the 700°C successively sintered case where the catalyst was cooled to 600°C in oxygen and reduction was started at 600°C. Catalysts were outgassed in flowing helium for 2 hr (successively sintered cases) or 1 hr (sepa-

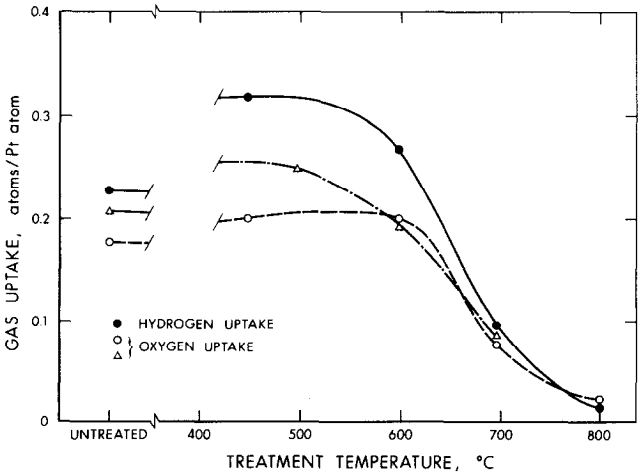


FIG. 2. Effect of treatment temperature on metal dispersion for 0.5% Pt on $Al_2O_3$ by gas uptake (see text for treatment conditions).

rately sintered cases) at 500°C before being cooled for gas uptake measurement. Use of the catalysts for other experiments prior to the sintering study may account for the 15% difference in initial oxygen uptake observed for the untreated catalyst samples.

At moderate sintering temperatures a redispersion of metal occurs for both catalysts. The increase in hydrogen uptake for the sample sintered at 450°C is far greater than the increase in oxygen uptake of the same sample. However, several authors (*17–19*) have noted that relative to oxygen, hydrogen uptakes increase as dispersion increases. Hence, for redispersion, particularly to very small Pt particles, larger increases in hydrogen uptake compared to oxygen would be expected.

It appears that changes in dispersion are strongly related to the atmosphere in which the catalyst is treated. For example, a portion of the 0.5% Pt on $Al_2O_3$ catalyst for which the oxygen uptake had been determined was used in another series of experiments, during which time it was exposed to flowing hydrogen at 500°C for a total of 10 hr and to flowing helium at 500°C for 22 hr. The subsequent oxygen uptake increased by only 0.004 atoms/Pt atom (2% of the total uptake) from the initial oxygen uptakes, a value of the order of the accuracy of the uptake measurement. Comparing this with the results in Fig. 2 indicates that dispersion changes are far more extensive for shorter treatment in oxygen, for which 16 hr treatment at 500°C gave a 19% increase in oxygen uptake.

### 2. *Variable Time/Constant Temperature Treatments*

Several samples of a second commercial catalyst (Engelhard 0.3% Pt on $Al_2O_3$) were treated in air at 575°C for varying time periods, from 6 hr to over 1 mo. Based on the results from overnight sintering reported above, it was felt that sintering at 575°C would provide a rate of change of dispersion sufficiently slow to allow monitoring of the kinetics. However, sintering was unexpectedly rapid; after 6 hr the uptake of oxygen had dropped from 0.350 atoms/atom Pt (for the unsintered specimen) to 0.019. At this low an uptake, gas adsorption measurements are subject to large relative error.

The unsintered catalyst was examined by electron microscopy, and metal particles were observed between 2 and 4 nm.

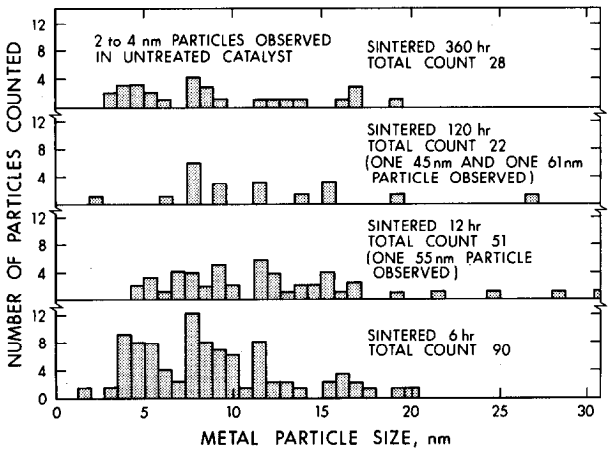


FIG. 3. Particle size distribution from electron micrographs of a sintered Englehard 0.3% Pt on $Al_2O_3$ catalyst. Batches were heated at 575°C in air for the indicated time.

Figure 3 shows the observed particle sizes for four of the sintered catalyst samples. The rapid growth of large metal particles even after a 6 hr sintering period is evident.

Comparison with the results of the earlier experiments involving the 0.5% Engelhard catalyst is difficult, however. Both catalysts are of the surface coated type, where the metal particles are in a thin layer on the outside of the alumina pellet. Thus while 0.3 and 0.5% are nominal metal loadings, the actual concentration of metal in the outer region is unknown and could vary substantially from one catalyst lot to another.

*3. Catalyst Mixture Experiments*

A series of experiments were designed to check the effect of addition of a small portion of heavily presintered catalysts on sintering kinetics. A portion of the 2.03% Pt on Alon alumina catalyst was heavily sintered (16 hr at 700°C in flowing oxygen) and had an oxygen uptake of 0.0313 atoms/Pt atom; examination of electron micrographs confirmed the presence of large metal particles (range observed, 2.5–27 nm). The fresh catalyst had an initial oxygen uptake of 0.256 atoms O/Pt atom.

Four batches of catalyst were then prepared; two of the fresh catalyst, and two of a mixture of 23.1 wt% of the heavily sintered catalyst and 76.9 wt% of the fresh catalyst. The batches of mixed catalyst were crushed, wetted and redried at 110°C to promote a thorough mixing of the sintered and unsintered portions. One mixed batch and one fresh batch were sintered 16 hr in flowing oxygen at 575°C and their oxygen uptakes were measured. These samples were subsequently sintered 16 hr at 610°C, while the other two batches were sintered 16 hr at 630°C. Samples were sintered, reduced (by cooling in flowing hydrogen from the sintering temperature to 500°C) and outgassed 1 hr (at 500°C in helium) under identical conditions; the sole exception was the mixed sample sintered at 610°C which was reduced and outgassed at 610°C.

Table 1 shows the initial oxygen uptakes for the four cases. The treatment at 575°C appeared to cause a slight redispersion in the samples. However, for the other two temperatures the mixed catalyst sinters significantly more extensively than the unmixed catalyst: after the 610°C treatment the unmixed catalyst had 66% of its original area compared to 43% for the mixed, after the 630°C treatment the unmixed catalyst had 29% of its original area compared to 3% for the mixed. From this data it appears that the presence of a portion of heavily sintered catalyst containing large metal particles speeds the sintering of a catalyst. The implications of this conclusion on proposed sintering mechanisms is discussed below.

Comparison of the results in Fig. 1 and Table 1 indicates a dependence of sintering behavior on metal loading for the prepared catalysts. The two Alon supported catalysts (4.76 and 2.03% Pt) were similarly prepared, but the more heavily loaded catalyst shows sintering at 550°C (growth of Pt particles up to 80 nm), while the less heavily loaded catalyst shows no significant change in dispersion after similar treatment at 575°C. Pt particles from 1

TABLE 1
EFFECT OF ADDITION OF A PORTION OF PRESINTERED CATALYST ON THE SINTERING RATE OF A 2.03% Pt ON ALON CATALYST

| Treatment | Oxygen uptake (atoms O/Pt atom) | |
|---|---|---|
| | Unmixed | Mixed |
| Unsintered | 0.256 | 0.204[a] |
| Sintered at: 575°C | 0.258 | 0.218 |
| 610°C | 0.169 | 0.087 |
| 630°C | 0.073 | 0.006 |

[a] By calculation from the dispersions of the unsintered and presintered samples.

to 3 nm were observed in the reduced 2.03% catalyst, compared to 1 to 4 nm for the reduced 4.76% catalyst.

*4. Effect of Reduction and Sintering on Individual Metal Particles*

Unreduced 2.03% Pt on Alon catalyst was deposited onto a specially prepared "holey" film described above. Benchmarks on the grid made it possible to record electron micrographs of the same area before reduction, after reduction, and after various thermal treatments in flowing helium. Table 2 lists the details of treatment for the grids.

While the intention of these experiments was to follow the effect of various treatments on representative catalyst areas, some cautions must be used before conclusions on these studies are drawn about catalyst sintering. In several important ways a catalyst supported on a holey carbon film mounted on a tungsten grid differs from a pure catalyst specimen. Other factors limit the accuracy of size and spatial position determinations of supported metal particles. For example:

a. Evidence appeared in about half the micrographs of small shifts (< 10 nm) in portions of the Alon substrate. In addition, a few micrographs showed evidence of major movements (> 10 nm) of the substrate. Thus the position of metal particles from micrograph to micrograph may in part be affected by movement in the substrate, arising from loss of $H_2O$ during the reduction step (the first time the catalyst is heated above 110°C) or the high temperatures realized in thermal treatment.

b. Crushing the catalyst and dropping it on the grid gave catalyst clumps of various size. In selecting an area to be examined, a balance had to be struck between very thin clumps of catalyst, where electron microscope imaging clarity was good but the amount of catalyst was low, and thick clumps, were imaging clarity was reduced but the catalyst more closely approximated the bulk typical in a sintered catalyst. The result was a compromise which often re-

TABLE 2
GRID TREATMENTS

| Grid | Areas examined | Treatment history[a] |
|---|---|---|
| 1 | 9 | Reduced at 300°C for 0.5 hr, some contamination noted; sintered 3 hr at 500°C (inserted in hot furnace), heavy contamination noted; film ruptured after further 3 hr at 500°C |
| 2 | 9 | Reduced at 300°C for 0.5 hr, some contamination noted; film ruptured after 5 hr sintering at 500°C |
| 3 | 4 | Reduced at 300°C for 0.5 hr, some contamination noted; film ruptured after 4 hr sintering at 500°C |
| 4 | 4 | Reduced at 300°C for 0.5 hr, heavy contamination noted; sintered 2.5 hr at 500°C, contamination reduced; film ruptured after 72 hr sintering at 550°C |
| 5 | 4 | Reduced at 300°C for 0.5 hr, deposits on grid noted (possibly Mo contamination from a previous experiment); grid discarded |
| 6 | 4 | Reduced at 300°C for 0.5 hr, some contamination noted; sintered 4 hr at 500°C, heavy contamination noted; sintered an additional 4 hr at 500°C, very heavy contamination noted; sintered 4 hr at 550°C, very heavy contamination noted |
| 7 | 3 | Reduced at 300°C for 0.5 hr, heavy contamination noted; sintered 4 hr at 500°C, some contamination noted; film ruptured after 4 hr sintering at 600°C |

[a] All sintering treatments in flowing helium started in cold furnace unless otherwise noted; all reductions in flowing hydrogen.

duced the quality of the image over what could be expected in ideal conditions. Where possible, thin regions at the edge of thick clumps were chosen, but this frequently led to a considerable range of elevation in the specimen, a factor which causes resolution and detection problems (*16*).

c. Contamination by carbon was far greater than that observed in conventional micrographs, both after reduction and after thermal treatment. There are two sources of carbon to contaminate the catalyst. One is from the cracking by the electron beam of residual hydrocarbon vapors within the microscope from the oil diffusion pump. However, under normal operation of the microscope with a liquid nitrogen filled "cold finger" in the area of the sample such contamination is quite low [see, for example, the micrographs in Refs. (*14* or *16*)]. The second source is the carbon in the film itself, which during reduction and sintering treatments may have migrated onto the catalyst from the film. Given the high contamination evident in many of the micrographs compared to conventional micrographs, we suspect this latter source to be significant; if so, then catalysts treated on grids differ from ordinary catalysts due to the presence of mobile or vaporized carbon.

d. Evidence from micrographs also suggests that platinum can migrate onto the carbon, and may accumulate there in preference to remaining on the alumina. Figure 4 (top) shows two micrographs of the same specimen area of grid 6 at relatively low magnification, before reduction and after the second thermal treatment. The large dark region in the lower left hand corner of Fig. 4 (top) appears to be a Pt crystal on the carbon. Similarly, Fig. 4 (bottom) shows three micrographs of another region of grid 6 before reduction and after the second and third thermal treatments. Not only are the development of metal deposits [in the areas (a), (b), (c) and (d) in Fig. 4 (bottom), for example] evident after sintering, but their growth or decay with increasing sintering is also demonstrated. Access by the migrating platinum to the carbon film, and possibly to the metal grid, is a second major difference between grid treated catalysts and ordinary samples.

With these cautions in mind, several observations about the growth of Pt particles on supported metal catalysts may be made from micrographs of the grid treated catalysts. (Photographic reproduction may have reduced the quality of the micrographs, especially for fine detail; prints of the original micrographs are available from the authors on request.)

In the unreduced catalyst the Pt is extremely disperse. While typically Pt particles with images corresponding to 2 nm were noted, comparison of a sintered and unreduced catalyst (for example, Fig. 5) shows that much of the Pt evident after sintering does not show up in the unreduced state, presumably because it is atomically dispersed and has not agglomerated into crystals. [In a previous work (*16*), we discussed the difficulty of relating image size to object size, particularly for detail smaller than 2.5 nm. All size measurements reported here are image sizes corrected for magnification, with a probable variance of up to $\pm 1$ nm from true object sizes.] In Fig. 6 larger Pt crystallites than normal appear in the unreduced catalyst; this will be discussed below.

Some agglomeration of Pt takes place during reduction of the catalyst; examination of Figs. 6, 7 and 8 illustrate this. In Fig. 6, despite heavy carbon contamination in the micrograph of the reduced catalyst, growth of the Pt clusters compared to the unreduced catalyst can be noted. In both Figs. 7 and 8 numerous larger particles up to 4 nm appear, and a general agglomeration of Pt is evident. This agglomeration is somewhat remarkable considering the mild temperatures

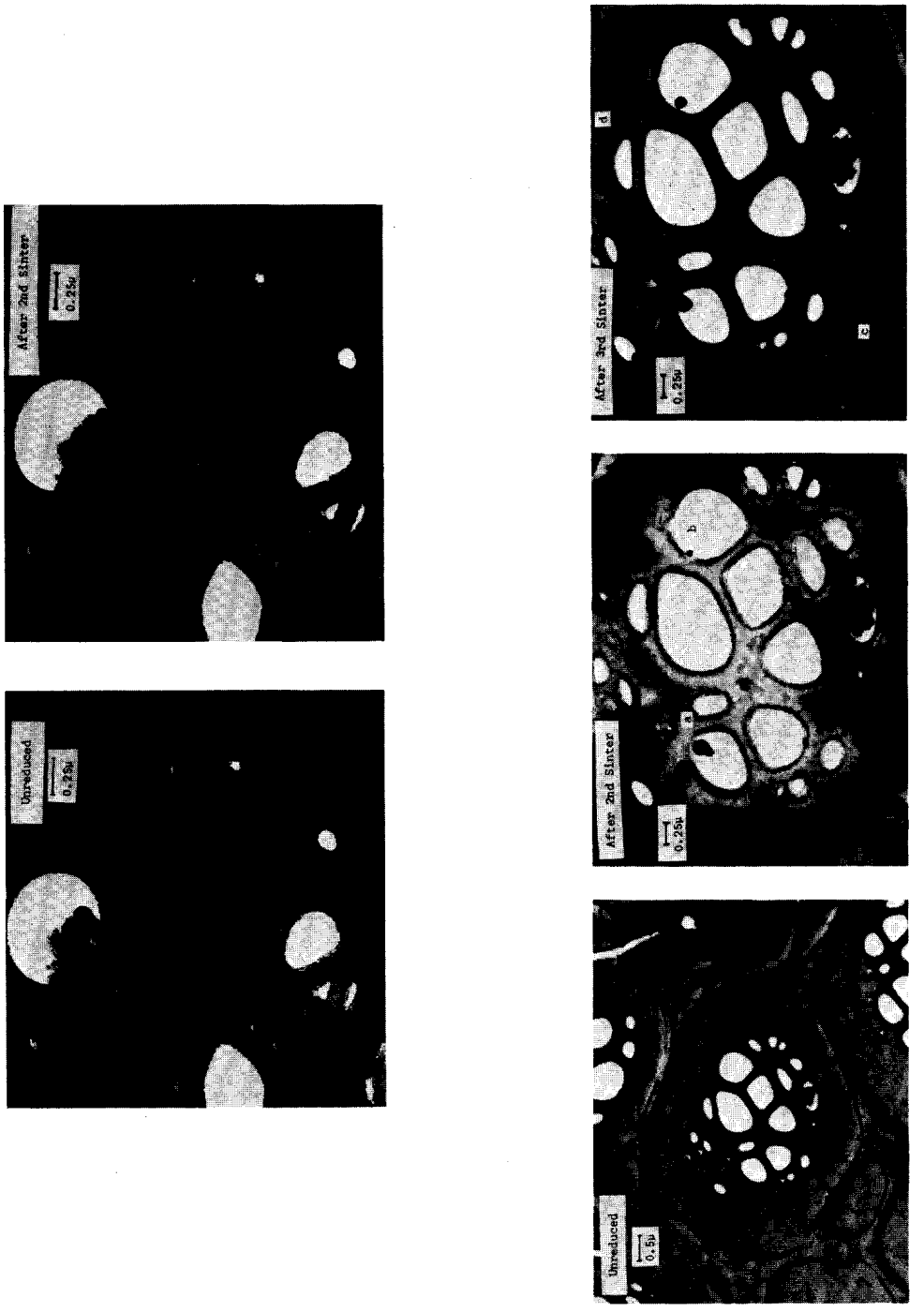


FIG. 4. Low magnification micrographs from grid 6 showing the accumulation of metal on the carbon film with successive thermal treatments.

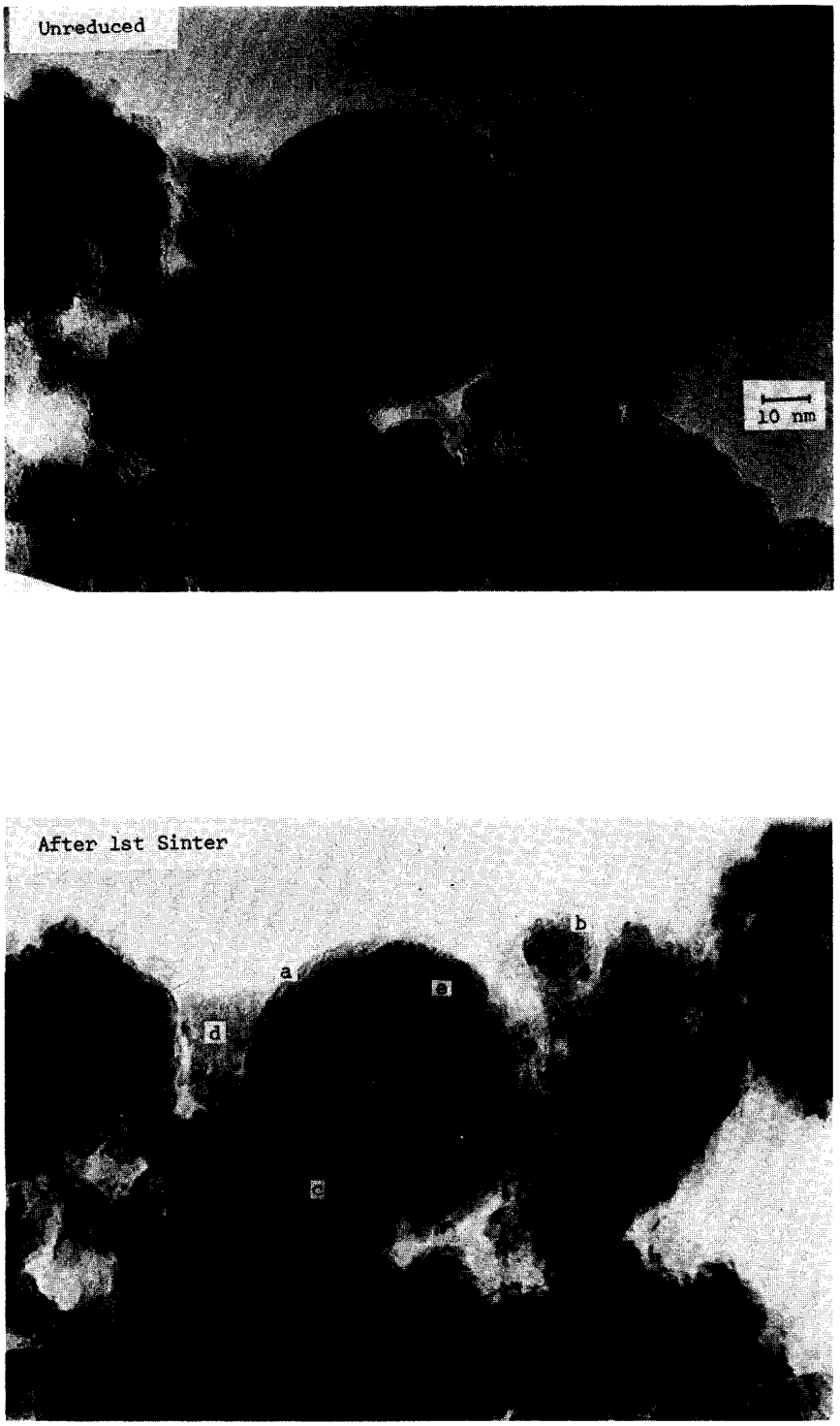


FIG. 5. Micrographs from grid 4 showing the same area before reduction and after one thermal treatment at 500°C.

(300°C) used in the reduction step. Close inspection of Figs. 7 and 8 show that some of the particles noted in the unreduced catalyst remain fixed in location during reduction. In Fig. 7, for example, five particles are illustrated [one each at (a), (b), and (c) and two at (d)] which appear in both micrographs. Similarly, two particles each by regions (a) and (b) in Fig. 8 appear before and after reduction. Not all particles in the reduced catalyst correspond to a particle in the unreduced catalyst; however, the small size of particles involved and the thickness of the specimen make simultaneous resolution of all small Pt particles unlikely (*16*).

Thermal treatment at 500°C leads to further agglomeration of Pt, as shown in Figs. 6 and 8. In Fig. 8, a consolidation of Pt particles is generally evident. In the region (c), a number of small particles evident in the reduced catalyst disappear and are replaced by one large (4 nm) particle in the sintered catalyst. A similar agglomeration is strikingly evident in Fig. 6, where particles of the order of 20 nm in size appear

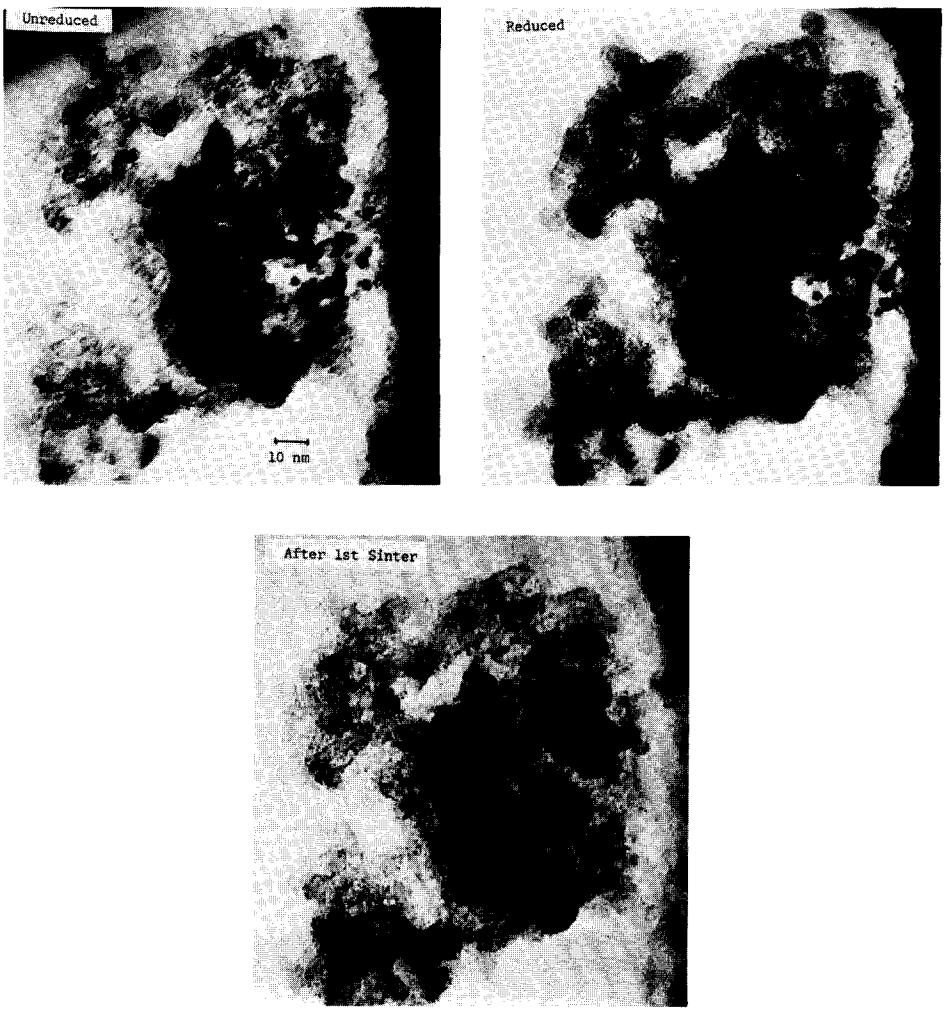


FIG. 6. Micrographs from grid 7 showing the same area before and after reduction and after one thermal treatment at 500°C.

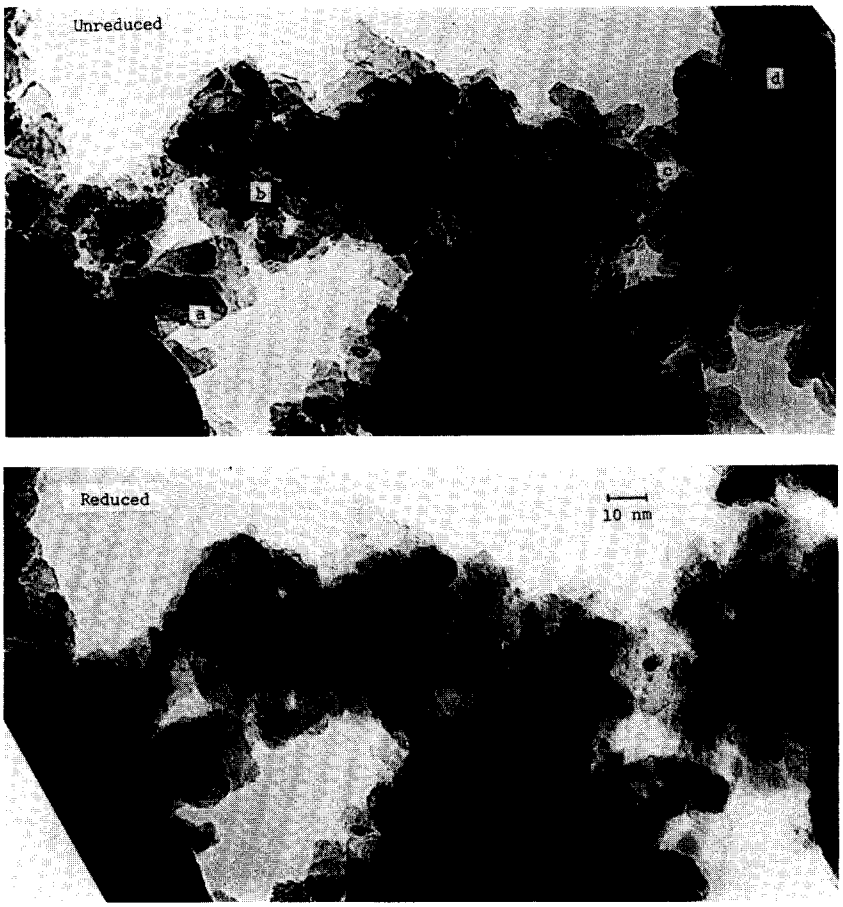


FIG. 7. Micrographs from grid 2 showing the same area before and after reduction.

after thermal treatment at 500°C. Once again, there is evidence of some particles remaining stationary during treatment. In Fig. 5, particles observed after thermal treatment at regions (a), (b), and (c) correspond to particles observed in the unreduced state. This is not true of all the particles in Fig. 5, however, such as those by (d) and (e). In these cases no particles are evident in the unreduced state, although the problem of detectability again exists for the very small unreduced particles. In Fig. 8, the two particles each in regions (a) and (b) again remain stationary during thermal treatment at 500°C, although two apparently new particles appear by (d).

Both Figs. 6 and 8 suggest that some localized effects are significant in the changes in metal particles associated with reduction and thermal treatments. For example, in Fig. 6 an unusually high density of Pt exists in the unreduced catalyst in the central area. While the reasons for this concentration of Pt salt are unknown, it results in Pt particles 5 to 10 times larger than normal after sintering. In light of the apparent influence of larger Pt crystallites on the overall sintering rate (see Sec. 3 above), such localized effects may be significant in the sintering of a catalyst. In Fig. 8, the apparent agglomeration of the particles in region (c) to the large particle

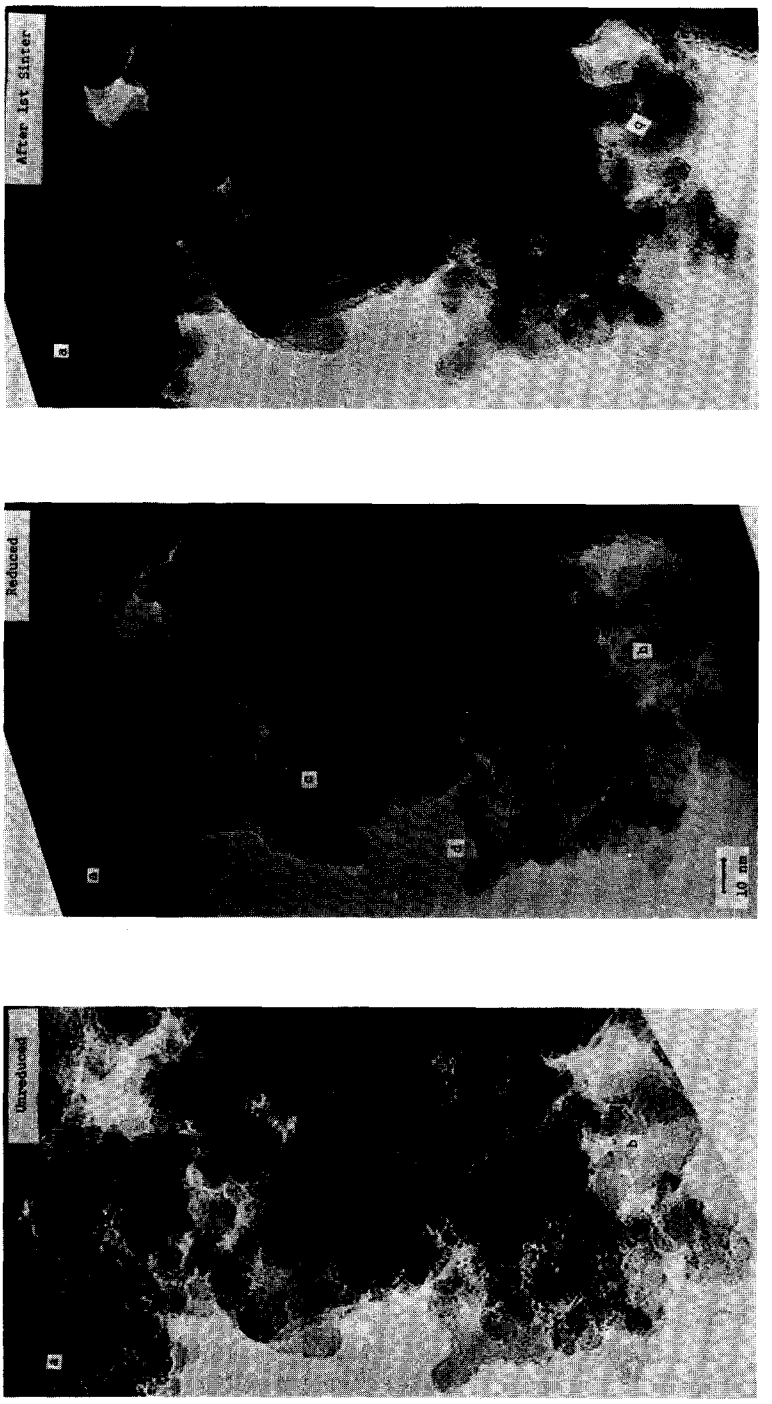


FIG. 8. Micrographs from grid 1 showing the same area before and after reduction and after one thermal treatment at 500°C.

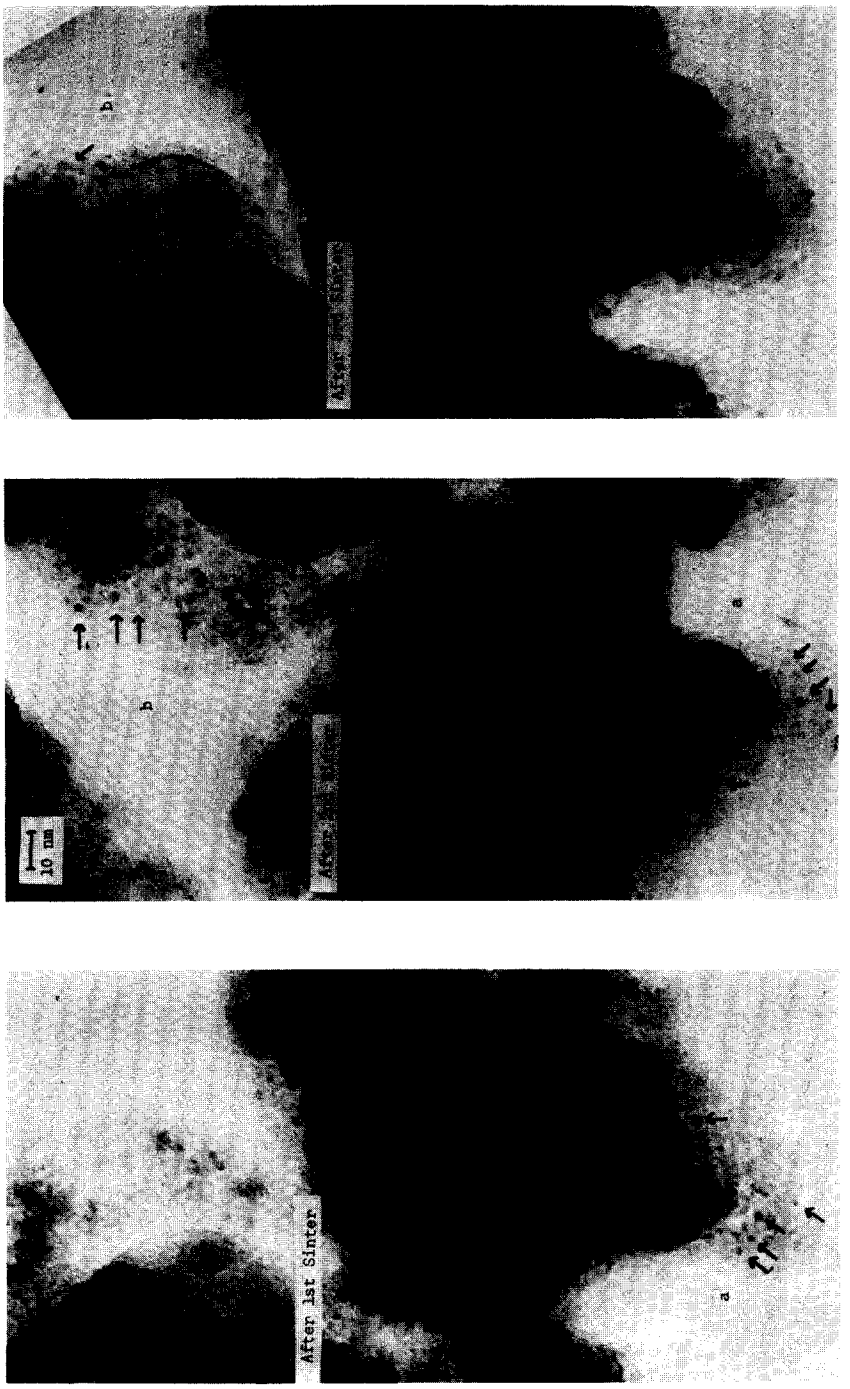


FIG. 9. Micrographs from grid 6 showing the same area after thermal treatment at 500°C, a second thermal treatment at 500°C, and a third treatment at 550°C.

evident after thermal treatment again suggests a localized effect due to the close proximity of so many Pt particles.

In only one case, grid 6, did the holey carbon film in the areas micrographed survive more than one sintering treatment. Figure 9 shows the same specimen area after three thermal treatments (the middle micrograph is the mirror image of the other two because the grid was inverted). The extremely high carbon contamination, evident in all three micrographs, makes the distinction of individual Alon particles impossible, and severely impedes the clarity of the Pt crystallites. Despite this problem, the continued agglomeration of Pt can be noted for increasing thermal treatments: typical particle sizes change from 2.5 to 5 nm. While the poor clarity limits particle detection, we were able to note that some particles did not shift with the thermal treatment. Six particles noted in region (a) after the first sinter were identified in the micrograph taken after the second sinter. Similarly, five particles evident after a third thermal treatment correspond to an existing particle in the same location prior to the treatment. The caution must also be reemphasized that the catalyst on grid 6, contaminated by carbon (presumably from the holey film), and losing metal to the film surface (shown in Fig. 4), deviates substantially from a typical $Pt/Al_2O_3$ catalyst system.

## DISCUSSION

The purpose of these experiments was in part to try to establish the mechanism of sintering, specifically to distinguish between crystallite migration (*12,13*) and atomic or molecular interparticle transport (*14,15*) as the sintering process. This pursuit is by no means of academic interest only, since knowledge of the mechanism of Pt agglomeration would suggest appropriate schemes to control or reverse the loss of metal dispersion. Unfortunately, we do not consider the evidence gathered in this work to be sufficiently definitive to allow elimination of one or the other mechanisms.

Sintering of the 4.76% Pt on Alon catalyst suggests strongly, however, that crystallite diffusion is not the sole mechanism of catalyst sintering, as previously noted (*14*). The Alon substrate consists of 10 to 30 nm alumina particles; upon drying these appear to form irregular porous stacking arrangements. As Fig. 1 shows, growth of Pt particles continues even when the metal crystallite size exceeds the size of a typical support particle; it is difficult to conceive of crystallite motion along the support surface continuing to occur in such a case.

Sintering of the commercial 0.5% Pt catalyst confirms the ability of supported metal catalysts to show an increase in dispersion (measured by gas uptake) with certain thermal treatments. Flynn and Wanke (*14,15*) account for redispersion as a transitory effect arising from the buildup of a high surface concentration of mobile metal species; cooling of a catalyst could "freeze" this metal as small crystallites or atomically dispersed atoms. Emilianova and Hassan (*20*) compared the dispersions of supported Pt catalysts which were rapidly and slowly cooled following otherwise identical thermal treatments. Their finding that the rapidly cooled catalyst always had a higher dispersion than the slowly cooled catalyst does support a "freezing" of the agglomeration process. Ruckenstein and Pulvermacher (*12,13*) do not account for redispersion in their model, but propose to do this in a future work, attributing it to particle breakup caused by a spreading surface pressure. Attempts to determine whether redispersion is a transitory phenomenon followed by particle growth were frustrated when the 0.3% Pt commercial catalyst showed an unexpectedly high rate of sintering at 575°C.

The higher rate of sintering observed when presintered catalyst containing large

Pt particles is added to a catalyst batch suggests that the large Pt particles speed agglomeration by acting as a "sink" for the transported metal. This in turn strongly suggests a highly mobile rapidly transported Pt species under the sintering conditions employed, since if the process were controlled by slowly diffusing Pt crystallites the effect of large metal particles on sintering rate would be minimal. The atomic diffusion model (*14,15*) assumes a very rapid migration of metal atoms or molecules along the substrate such as is noted in film growth studies (*21*). Ruckenstein and Pulvermacher (*12,13*) describe a coalescence controlled condition, in which the rate of merger of metal particles is slower than their migration along the surface. However, Wynblatt and Gjostein (*9*) consider a sintering rate being coalescence controlled as impossible. If so, this suggests interparticle transport rather than crystallite migration as a sintering mechanism that can account for the influence of the added large Pt particles on the overall sintering rate.

An ideal way of distinguishing between crystallite migration and atomic diffusion mechanisms would be to sinter a catalyst while observing it in the electron microscope, using a heated grid holder. However, our attempts at this were frustrated because drift of the specimen, presumably due to thermal gradients in the grid, prevented resolution and recording of the metal particles of the order of 10 nm and less. The selection of an area of catalyst, to be examined after various treatments, was intended to approximate as closely as possible the *in situ* experiment. However, two detectability problems affected the electron micrograph studies of catalysts treated on grids. For small particles, the problem of simultaneous detection of all Pt crystallites (*16*) arises. For larger particles, carbon contamination, which we think arises from evaporation from the holey carbon film during thermal treatment, reduces the clarity of the micrographs. We conclude that at least some Pt particles remain in a fixed location during reduction and continued thermal treatments, and that agglomeration of Pt occurs during all of these steps. For a perfectly homogeneous surface, the crystallite migration model of sintering (*12,13*) predicts all Pt particles will move, while the atomic surface diffusion model predicts none will (although some will disappear). On a heterogeneous surface, however, which probably more accurately describes a typical catalyst support, the former model can account for fixed particles and the latter can account for the appearance of particles at new locations. Hence these EM studies do not allow either model to be definitively selected.

Contamination of the catalyst by material from the supporting grid would probably be reduced or disappear if a high boiling metal (such as tungsten) holey support film were used; Fukami *et al.* (*22,23*) describe the preparation of these films. However, this would probably not reduce the transport of Pt to the support film, shown in Fig. 4.

## CONCLUSIONS

Sintering of supported metal catalysts was studied in a variety of experiments. For a 4.76% Pt on Alon catalyst, metal particle growth continued to a point where it exceeded the particle size of the support. Sintering of Englehard 0.5% Pt on alumina catalysts in oxygen gave evidence of redispersion at lower temperatures (450–600°C) and loss of metal surface at higher temperatures (>600°C). The rate of sintering was found to be sensitive to the gas atmosphere and to the metal loading.

Including a portion of presintered catalyst in a catalyst batch to be sintered appears to substantially increase the overall rate of sintering. This is attributed to the large Pt particles found in the presintered

specimen acting as a "sink" for transported metal.

Electron micrographs were recorded of the same catalyst area before reduction and after reduction and thermal treatments on the grid. Problems were noted with metal transport to the grid carbon support film and carbon transport to the catalyst. Agglomeration of Pt was noted after reduction in hydrogen at 300°C and after thermal treatments in helium at 500 and 550°C. Some metal particles kept a fixed location on the support during reduction and thermal treatments.

The data can be interpreted in terms of an interparticle transport sintering mechanism. While some of the data cast doubt upon crystallite migration as a sintering mechanism, we do not consider the results sufficiently conclusive to rule out this model as a possible mechanism of sintering.

## ACKNOWLEDGMENTS

One of us (P.C.F.) gratefully acknowledges the support of an International Nickal Company Graduate Fellowship. We also appreciate the support of this research by the National Research Council of Canada. The Alon used was kindly donated by the Cabot Corporation.

## REFERENCES

1. *Chem. Abstr.* **76,** 145405q (1972) (*Pat., Ger. Offen.* 2, 137, 554).
2. *Chem. Abstr.* **68,** 31814b (1968) (*Pat., Neth. Appl.* 6, 614, 074).
3. Herrmann, R. A., Adler, S. F., Goldstein, M. S., and De Baun, R. M., *J. Phys. Chem.* **65,** 2189 (1961).
4. Maat, H. J., and Moscou, L., *Proc. Int. Congr. Catal., 3rd, 1964* p. 1277 (1965).
5. Somorjai, G. A., *in* "X-Ray and Electron Methods of Analysis" (H. van Olphen and W. Parrish, Eds.), Chap. 6. Plenum, New York, 1968.
6. Wynblatt, P., and Gjostein, N. A., *Scr. Met.* **7,** 969 (1973).
7. Gruber, H. L., *J. Phys. Chem.* **66,** 48 (1962).
8. Hughes, T. R., Houston, R. J., and Sieg, R. P., *Ind. Eng. Chem. Process Des. Develop.* **1,** 96 (1962).
9. Wynblatt, P., and Gjostein, N. A., *Progr. Solid State Chem.* **9,** in press.
10. Huang, F. H., and Li, C. Y., *Scr. Met.* **7,** 1239 (1973).
11. Gregg, S. J., and Howlett, B. J., *SCI (Soc. Chem. Ind., London Monogr.)* **28,** (1968).
12. Ruckenstein, E., and Pulvermacher, B., *AIChE J.* **19,** 356 (1973).
13. Ruckenstein, E., and Pulvermacher, B., *J. Catal.* **29,** 224 (1973).
14. Flynn, P. C., and Wanke, S. E., *J. Catal.* **34,** 390 (1974).
15. Flynn, P. C., and Wanke, S. E., *J. Catal.* **34,** 400 (1974).
16. Flynn, P. C., Wanke, S. E., and Turner, P. S., *J. Catal.* **33,** 233 (1974).
17. Kikuchi, E., Flynn, P. C., and Wanke, S. E., *J. Catal.* **34,** 132 (1974).
18. Wilson, G. R., and Hall, W. K., *J. Catal.* **17,** 190 (1970).
19. Dalla Betta, R. A., and Boudart, M., *Proc. Int. Congr. Catal., 5th, 1972* **2,** *96*-1329 (1973).
20. Emelianova, G. I., and Hassan, S. A., *Proc. Int. Congr. Catal., 4th, 1968,* p. 1329, (1969).
21. Geus, J. W., *in* "Chemisorption and Reactions on Metallic Films" (J. R. Anderson, Ed.), Chap. 3. Academic Press, London, 1971.
22. Fukami, A., and Adachi, K., *J. Electronmicrosc.* **14,** 112 (1965).
23. Fukami, A., Adachi, K., and Katok, M., *J. Electronmicrosc.* **21,** 19 (1972).